Consistency between continuous and discrete models – Another modeling problem in numerical simulation procedure –

AISO, Hideaki *

In the procedure of numerical simulation, which is widely used in science and engineering research and development activities, there are two stages of modeling. First we describe the phenomenon that we simulate by mathematical equations. It is called mathematical modeling. The mathematical description is usually a kind of continuous model including the concept of infinity or limiting etc., *i.e.* differentiation, integral and so on. Then we need the second modeling that approximates the continuous model by some discrete model that can be directly made into a computer program and computed by digital computers.

While the word "modeling" usually means the mathematical modeling, the second modeling is also an important factor in establishing the reliability of numerical methods and it is expected to realize some enough consistency between the continuous and discrete models. The lack of consistency between both models might even do harm with the discussion on the mathematical modeling.

We are concerned with the second modeling. We here discuss a few consistency (and inconsistency) problems that happen when the compressible Euler equations are discretized by differencing

1. Introduction

From the word of modeling almost all the people may imagine how to describe by mathematical equations the target phenomenon or machinery that we aim to analyze or optimize. Such mathematical description is called mathematical model and the procedure to obtain the equations is called mathematical modeling.

But in numerical simulation technology using digital computers we usually need another kind of modeling. The equations obtained through the mathematical modeling are usually continuous models like partial differential equations, which includes mathematical concepts of differentiation, integral and so on. The equations of continuous models can not be directly translated into the computer programs. Therefore we approximate the equation of continuous models by discrete equation using finite difference method, finite element method or other discretization methods and compute the discrete equation by digital computer. The obtained discrete equation is called discrete model and the discretization is another modeling to obtain the discrete models from then continuous ones.

Between the both models we naturally expect the consistency which means that the discrete model should inherit the property of the original continuous model. But it sometimes happens that the discrete model includes some fake property that does not come from the continuous model or that some essential property of continuous model is missed in the discrete model. Such inconvenience is called inconsistency between the both models. The complete consistency is usually impossible and some inconsistency is inevitable because the continuous and discrete models are different things that belongs to different categories. Then we require the discrete models' inheritance of essential property to establish reli-

*IAT (Institute of Aerospace Technology), JAXA (Japan Aerospace eXploration Agency) Jindaiji-Higashi-machi 7-44-1 Chofu TOKYO 182-8522 JAPAN, aiso@chofu.jaxa.jp

able numerical simulation. What is essential may vary according to the purpose of numerical simulation even if the same continuous model is used, and the required consistency may vary as well.

Such consistency-inconsistency problems as above are usually mathematical problems. Conventional viewpoint is that how well the discrete model approximates the continuous model, but it is also important to analyze the property or behavior of both models in parallel and compare them. In the case of partial differential equations for the motion of fluid, where the theory of exact solution is not enough, we especially need to discuss the property of discrete model from the viewpoint of consistency and inconsistency with the continuous model to improve the reliability of numerical simulation.

In this article we show and discuss a few inconsistency problems when the compressible Euler equations are discretized by Godunov method.

2. Compressible Euler Equations.

We are here concerned with difference approximation for the compressible Euler equations. We restrict ourselves into the one and two dimensional cases.

The one dimensional compressible Euler equations is written as follows.

$$U_t + F(U)_x = 0, -\infty < x < \infty, t > 0 \quad (1)$$

where $U = U(x,t)$, a function of space variable x and time t, is the vector of conservative variables

$$U = \begin{bmatrix} \rho \\ \rho u \\ e \end{bmatrix}$$

with the density ρ, the velocity u, the total energy e per unit, and F is the flux

$$F = \begin{bmatrix} \rho u \\ \rho u^2 + p \\ u(e+p) \end{bmatrix}$$

with the pressure p. U_0 is the initial value.

Similarly, the two dimensional problem is written in the form

$$U_t + F(U)_x + G(U)_y = 0, \quad -\infty < x, y < \infty, t > 0 \quad (2)$$

where the vector $U = U(x,y,t)$ of conservative variables and the fluxes F and G in x- and y-directions, respectively, are

$$U = \begin{bmatrix} \rho \\ \rho u \\ \rho v \\ e \end{bmatrix}, \ F = \begin{bmatrix} \rho u \\ \rho u^2 + p \\ \rho uv \\ u(e+p) \end{bmatrix}, \ G = \begin{bmatrix} \rho v \\ \rho uv \\ \rho v^2 + p \\ v(e+p) \end{bmatrix}.$$

u and v are velocity components in x- and y-directions, respectively.

We also assume the equation of state for ideal gas,

$$e = \frac{p}{\gamma - 1} + \frac{\rho u^2}{2} \text{ or } e = \frac{p}{\gamma - 1} + \frac{1}{2}\rho(u^2 + v^2), \quad (3)$$

where γ is the adiabatic constant.

3. Godunov method

While various methods of differencing the compressible Euler equations are proposed and each of them has its own advantage and disadvantage, we restrict our interest into Godunov method. It is one of the most naturally constructed difference methods with the use of finite volume concept and Riemann problem, although the cost of computation is not so cheap. Therefore it is a aimple and basic method in the theoretical sense and it is an appropriate discrete model to discuss the consistency problem between the continuous and discrete models.

Godunov method is finite volume scheme. First we discretize the space. We assume a discretization of uniform mesh. In one dimensional case $(-\infty, \infty)$ is discretized by the family $\{I_i\}_{i:\text{all the integers}}$ of finite volumes, where

$$I_i = (x_{i-\frac{1}{2}}, x_{i+\frac{1}{2}}),$$

$x_{i+\frac{1}{2}} = (i + \frac{1}{2})\Delta x$ with a space discretization increment Δx. In the two dimensional case $(-\infty, \infty) \times (-\infty, \infty)$ is discretized by $\{I_{i,j}\}_{i,j:\text{all the integers}}$, where

$$I_{i,j} = ((i-\frac{1}{2})\Delta x, (i+\frac{1}{2})\Delta x) \times ((j-\frac{1}{2})\Delta y, (j+\frac{1}{2})\Delta y),$$

$x_{i+\frac{1}{2}} = (i + \frac{1}{2})\Delta x$, $y_{j+\frac{1}{2}} = (j + \frac{1}{2})\Delta y$ with space discretization increments Δx and Δy in x- and y-

directions, respectively. The temporal discretization is given by $\{t^n\}_{n:\text{integers},n\geq 0}$, $t^n = n\Delta t$. Let U_i^n or $U_{i,j}^n$ an approximate value of the avarage of U

$$U_*^n = \frac{1}{I_*}\int_{I_*} U$$

over each finite volume I_i or $I_{i,j}$ at the time t^n. Using the law of conservation, the temporal evolution of integral of U over each volume I_i or $I_{i,j}$ is calculated as the sum of fluxes going across the boundary of the volume I_i or $I_{i,j}$ during the considered time. Then the finite volume scheme of difference is written in the following general form,

$$U_i^{n+1} = U_i^n - \frac{\Delta t}{\Delta x_i}\left\{\bar{F}^n_{i+\frac{1}{2}} - \bar{F}^n_{i-\frac{1}{2}}\right\} \tag{4}$$

in the one dimensional case, or

$$\begin{aligned} U_{i,j}^{n+1} = U_{i,j}^n - \tfrac{\Delta t}{\Delta x_i}\left\{\bar{F}^n_{i+\frac{1}{2},j} - \bar{F}^n_{i-\frac{1}{2},j}\right\} \\ - \tfrac{\Delta t}{\Delta y_j}\left\{\bar{G}^n_{i,j+\frac{1}{2}} - \bar{G}^n_{i,j-\frac{1}{2}}\right\}, \end{aligned} \tag{5}$$

in the two dimensional case, where $\bar{F}^n_{i+\frac{1}{2}}$, $\bar{F}^n_{i+\frac{1}{2},j}$, $G^n_{i,j+\frac{1}{2}}$ are numerical fluxes crossing the boundaries between I_i and I_{i+1}, $I_{i,j}$ and $I_{i+1,j}$, $I_{i,j}$ and $I_{i,j+1}$, respectively.

Godunov method employs the exact solution of Riemann problem naturally given at each boundary between neighboring finite volumes at each time step. In the one dimensional case a Riemann problem

$$\left\{\begin{array}{l} U_t + F(U)_x = 0 \\ U(x,0) = \left\{\begin{array}{l} U_i^n, x < 0 \\ U_{i+1}^n, x > 0 \end{array}\right. \end{array}\right. \tag{6}$$

is given. The problem has a self-similar exact solution $U = U(x,t;U_i^n,U_{i+1}^n) = U(x/t;U_i^n,U_{i+1}^n)$. In Godunov method the numerical flux crossing the boundary between I_i and I_{i+1} during the time interval $[t^n, t^{n+1})$ is given by

$$\bar{F}^n_{i+\frac{1}{2}} = F(U(0;U_i^n,U_i^n)) \tag{7}$$

and (4) and (7) determine the scheme of temporal evolution. In the two dimensional case, the numerical flux $\bar{F}^n_{i+\frac{1}{2},j}$ and $\bar{G}^n_{i,j+\frac{1}{2}}$ are given by

$$\bar{F}^n_{i+\frac{1}{2},j} = F(U(0;U_{i,j}^n;U_{i+1,j}^n)), \tag{8}$$

$$\bar{G}^n_{i,j+\frac{1}{2}} = G(U(0;U_{i,j}^n;U_{i,j+1}^n)) \tag{9}$$

using the solution to Riemann problems

$$\left\{\begin{array}{l} U_t + F(U)_x = 0 \\ U(x,0) = \left\{\begin{array}{l} U_i^n, x < 0, \\ U_{i+1}^n, x > 0, \end{array}\right. \end{array}\right. \tag{10}$$

$$\left\{\begin{array}{l} U_t + F(U)_x = 0 \\ U(x,0) = \left\{\begin{array}{l} U_i^n, x < 0, \\ U_{i+1}^n, x > 0, \end{array}\right. \end{array}\right. \tag{11}$$

respectively.

Unfortunately, in the case of compressible Euler equations the existence and uniqueness of exat solution is still an open problem, and any difference scheme is not proved to converge to the exact solution in any sense. But it might be expected that Godunov method would be one of the converging difference schemes if some difference schemes could be proved to converge to the exact solution.

In the following sections, we discuss a few inconvenient numerical behaviors of Godunov method. They may happen regardless with the sizes of difference increments. But the behaviors are those of discrete model and they do not necessarily prevent the scheme from convergencs as the difference increments tend to zero. On the contrary a difference scheme may still admit such kind of inconveniences even if its convergence proof is given.

4. Numerical instability around a strong shock wave.

It has been recognized from a time even before the article [2)] that mentions it first that some strange instability may occur in the numerical computation for compressible Euler equations when strong shock waves are formed. The instability is called *carbuncle phenomenon* or *carbuncle instability.* [2)] gives discussion from the viewpoint that the instability is from difference schemes.

From the experience, we already know some facts on the carbuncle instability. The instability occurs only in the case of multidimensional computation, even though the flow phenomenon

is sometimes only one-dimensional. The instability occurs when the shock surface is almost parallel to some axis of computational coordinate, but it seldom occurs when the shock surface is oblique enough to any of the axes. The stronger the shock, the more likely the instability occurs. The scale of instability has similarity to the size of computational grids, which implies that the instability comes from discrete models used in numerical computation but not from the original PDE.[1]

In [3], Moschetta et al. try to analyze the instability by comparing the linear stability of "large" system including all the variables in the computation and the occurrence of carbuncle instability in the real computation that is nonlinear. They do it in the case of stable shock that does not move in physical phenomenon, and they test a few kinds of difference schemes by using numerical derivative method to obtain each element of matrix of the "large" linear system.

In this section we observe the correspondence between some linearlized analysis and the occurrence of carbuncle instability in the case of progressing shock wave.

4.1. Numerical computation of progressing shock wave

We are concerned with the numerical computation of progressing shock wave.

We consider the initial value problem (2) with the initial value

$$U(x,0) = \begin{cases} U_L =^t [\rho_L, \rho_L u_L, 0, e_L], & x < 0, \\ U_R =^t [\rho_R, \rho_R u_R, 0, e_R], & x > 0 \end{cases} \tag{12}$$

that satisfies the Rankine-Hugoniot condition

$$F(U_R) - F(U_L) = s(U_R - U_L). \tag{13}$$

U_L and U_R are the states of both sides of planar shock parallel to y-axis progressing at the velocity s. For the physical relevancy of shock we assume the following entropy condition

$$u_L - c_L > s > u_R - c_R \text{ or } u_L + c_L > s > u_R + c_R \tag{14}$$

where $c_L = \sqrt{\gamma p_L/\rho_L}$ and $c_R = \sqrt{\gamma p_R/\rho_R}$ are the sound speeds of both side. We also assume the situation is always "fully upwind enough ";

$$u \pm c, u >> 0, c = \sqrt{\gamma p/\rho} \tag{15}$$

everywhere. Then the initial value problem (2), (12) has an entropy solution;

$$U(x,y,t) = U(x - st, y, 0) = \begin{cases} U_L, & x < st, \\ U_R, & x > st. \end{cases} \tag{16}$$

It means a progressing planar shock.

This solution is numerically calculated by Gudonov method. We impose the following CFL restriction

$$\frac{|u| + c}{\Delta x} + \frac{|v| + c}{\Delta y} \leq \frac{1}{\Delta t}. \tag{17}$$

4.2. Analysis on practical model of computation

We analyze the discrete temporal evolution (**??**) by Godunov method to examine the machinery that causes the carbuncle.

No carbuncle occurs if the initial data $\left\{U^0_{i,j}\right\}_{i,j}$ never depends on j and the discrete temporal evolution (**??**) is exactly calculated without any error. Even with errors, no carbuncle should not occur if the error at each cell $I_{i,j}$ does not depend on j.

In practical computation the errors at cells I_{i,j_1} and I_{i,j_2} might be different if $j_1 \neq j_2$.[2]

But the simple accumulation of such error is not enough to cause the carbuncle of our interest because, once any small carbuncle is recognized, it grows much faster than expected from the simple accumulation of error. Therefore it

[1] There are several different kinds of phenomena called "carbuncle". We restrict the statement only into the case of carbuncle mentioned above.

[2] It might come from the round off error in the digital representation of $\Delta y = y_{j+\frac{1}{2}} - y_{j-\frac{1}{2}}$. In fact, if we take $y_j + \frac{1}{2} = j$ as variables of "integer"-type, there is no difference of round off error at the cells $I_{i,j}$ of the same i and no carbuncle occurs. It is easily observed. But, also in this case, the instability may occur once a very small perturbation is artificially given.

is thought that the discrete temporal evolurion includes some machinery to amplify the error. Some other articles, for example, [3,1)] etc. also give discussion from a similar viewpoint.

For simplicity of analysis, we restrict the error into the exact odd-even mode;

$$\begin{aligned} &U^n_{i,j} = U^n_i + (-1)^j \hat{U}^n_i, \\ &U^n_i =^t [\rho^n_i, (\rho u)^n_i, 0, e^n_i], \\ &\hat{U}^n_i =^t [\hat{\rho}^n_i, (\widehat{\rho u})^n_i, (\widehat{\rho v})^n_i, \hat{e}^n_i]. \end{aligned} \tag{18}$$

The assumption is not so artificial. As mentioned in [2)], the carbuncle is almost odd-even. Furthermore, when the calculation is controlled like the footnote 2, a perturbation of the exact odd-even mode triggers the instability satisfying (18). But such control changes the property of instability very little.

The following theorem is basic in the analysis.

Theorem 1. *Asume the Godunov method. We obtain*

$$\begin{aligned} &\hat{U}^{n+1}_i \\ &= \hat{U}^n_i - \frac{\Delta t}{\Delta x}\left\{\frac{\partial F}{\partial U}(U^n_i)\hat{U}^n_i - \frac{\partial F}{\partial U}(U^n_{i-1})\hat{U}^n_{i-1}\right\} \\ &\quad - \frac{\Delta t}{\Delta y}\cdot 2\left|\frac{\partial G}{\partial U}(U^n_i)\right|\hat{U}^n_i + o(\delta) \\ &= \left\{I - \frac{\Delta t}{\Delta x}\frac{\partial F}{\partial U}(U^n_i) - 2\frac{\Delta t}{\Delta y}\left|\frac{\partial G}{\partial U}(U^n_i)\right|\right\}\hat{U}^n_i \\ &\quad + \frac{\Delta t}{\Delta x}\frac{\partial F}{\partial U}(U^n_{i-1})\hat{U}^n_{i-1} + o(\delta), \end{aligned} \tag{19}$$

or, in another expression,

$$\begin{aligned} &\frac{\partial U^{n+1}_i}{\partial U^n_i} = \left\{I - \frac{\Delta t}{\Delta x}\frac{\partial F}{\partial U}(U^n_i) - 2\frac{\Delta t}{\Delta y}\left|\frac{\partial G}{\partial U}(U^n_i)\right|\right\}, \\ &\frac{\partial U^{n+1}_i}{\partial U^n_{i-1}} = \frac{\Delta t}{\Delta x}\frac{\partial F}{\partial U}(U^n_{i-1}), \\ &\frac{\partial U^{n+1}_i}{\partial U^n_k} = O,\ i-k \neq 0, 1 \end{aligned} \tag{20}$$

where $|A|$ is determined for a diagonalizable matrix A by

$$\begin{aligned} |A| &= P\cdot diag(|\lambda_1|, |\lambda_2|, \cdots, |\lambda_n|)\cdot P^{-1} \\ &= P\begin{bmatrix} |\lambda_1| & 0 & 0 & \cdots & 0 \\ 0 & |\lambda_2| & 0 & \cdots & 0 \\ & \cdots & \cdots & \cdots & \\ 0 & & \cdots & & |\lambda_n| \end{bmatrix} P^{-1} \end{aligned} \tag{21}$$

with the diagonalization $P^{-1}AP = diag(\lambda_1, \lambda_2, \cdots, \lambda_n)$ with some matrix P.[3]

The proof is straightforward by the following lemmas 1 and 2. They are from the assumption (15) of full upwindness in x-direction and the fact that the flow in y-direction is almost acoustic.

Lemma 1.

$$\bar{F}^n_{i+\frac{1}{2},j} = F(U^n_{i,j}). \tag{22}$$

Lemma 2.

$$\begin{aligned} \bar{G}^n_{i,j+\frac{1}{2}} &= \tfrac{1}{2}\{G(U^n_{i,j}) + G(U^n_{i,j+1})\} \\ &\quad - \tfrac{1}{2}\left|\frac{\partial G}{\partial U}(U^n_i)\right|(U^n_{j+1} - U^n_j) + o(\delta). \end{aligned} \tag{23}$$

The both lemmas are easily proved by observing the observation of Riemann problem (**??**) or (**??**) to determine the numerical flux $\bar{F}^n_{i+\frac{1}{2},j}$ or $\bar{G}^n_{i,j+\frac{1}{2}}$, respectively.

Let $\hat{U}^n =^t [\cdots, \hat{\rho}^n_i, (\widehat{\rho u})^n_i, (\widehat{\rho v})^n_i, \hat{e}^n_i, \hat{\rho}^n_{i+1}, (\widehat{\rho u})^n_{i+1}, (\widehat{\rho v})^n_{i+1}, \hat{e}^n_{i+1}, \cdots]$. Determine the infinite matrix E^{n+1}_n by $E^{n+1}_n = \left[\frac{\partial U^{n+1}_i}{\partial U^n_k}(U^n_k)\right]_{i,k:\text{integers}}$, where each $\frac{\partial U^{n+1}_i}{\partial U^n_k}(U^n_k)$ is submatrix of the size 4×4 and indices i, k move over all the integers. Then $\hat{U}^n \mapsto \hat{U}^{n+1}$ is described as $\hat{U}^{n+1} = E^{n+1}_n \cdot \hat{U}^n + o(\delta)$. With the matrix E^{n+r}_n determined by $E^{n+1}_n = \left[\frac{\partial U^{n+r}_i}{\partial U^n_k}(U^n_k)\right]_{i,k:\text{integers}}$, $\hat{U}^{n+r} = E^{n+r}_n \cdot \hat{U}^n + o(\delta)$. Note $E^{n+r}_n = E^{n+r}_{n+r-1}\times\cdots\times E^{n+1}_n$, $r \geq 1$ and $\frac{\partial U^{n+r}_i}{\partial U^n_k}(U^n_k) = 0$ unless $i - r \leq k \leq i$.

We discuss the relation between the carbuncle and the linear stability of the map $\hat{U}^n \mapsto \hat{U}^{n+r} = E^{n+r}_n$ using discrete stable profiles of progressing shocks[4], which is explained in the beginning of next section. Our main insist is the following.

Insist. *The occurrence of carbuncle instsbility coincides with the linear instability of the map $\hat{U}^n \mapsto \hat{U}^{n+r}$*

4.3. Numerical experiments

There are two parts; preparing the profile of shock and seeing the instability.

[3] $|A|$ does not depend on P,the matrix used for diagonalization.

[4] The existence of such discrete stable profile of progressing shock is still open in theory. But it seems possible to obtain such profile numerically. It is discussed further in the next section.

4.3.1. Computation of profile

First we prepare a discrete stable profile of progressing shock numerically.

1. We use Godunov method for one dimension;
$$U_i^{n+1} = U_i^n - \frac{\Delta t}{\Delta x}\left\{\bar{F}^n_{i+\frac{1}{2}} - \bar{F}^n_{i-\frac{1}{2}}\right\}. \quad (24)$$
U_i^n's are those assumed in (18). $\frac{\Delta t}{\Delta x}$ is the same as that in the two dimensional computation later.

2. The computation domain is given by $i_{\min} \le i \le i_{\max}$ so that $i_{\max} - i_{\min}$ is large enough, and the initial values U_i^0's are given by
$$U_i^0 = \begin{cases} U_L, & i_{\min} \le i \le i_s \\ U_R, & i_s < i \le i_{\max}, \end{cases} \quad (25)$$
where U_L and U_R satisfy (13), (14), (15) and (17), and the shock speed s has a rational ratio to $\frac{\Delta x}{\Delta t}$, *i.e.* $s = \frac{q}{r} \cdot \frac{\Delta x}{\Delta t}$, q, r are positive integers relatively prime. The boundary is treated by the inflow condition at $i_{\min}$ and by the outflow condition at $i_{\max}$.

3. Proceed the discrete temporal evolution by (24).

4. Our goal is to obtain some stable profile of progressing shock. To do it within a limited domain, we shift the data every r steps of discrete temporal evolution, *i.e.* when $n \equiv 0 (\mathrm{mod} r), n > 0$, we shift back the data $\{U_i^n\}$ by r spatial nodes;
```
do i = i_min, i_max - q
  U_i^n = U_{i+q}^n
enddo
do i = i_max - q + 1, i_max
  U_i^n = U_R
enddo
```

5. Obtain the "convergence" of profile. Thanks to the data shift, in practical computation we can do it by comparing U_i^{n+r}'s and U_i^n's, for example, monitoring
$$S(n) = \sum_{i=i_{\min}}^{i_{\max}-r} \Big\{ |\rho_i^{n+r} - \rho_i^n| + |(\rho u)_i^{n+r} - (\rho u)_i^n| + |e_i^{n+r} - e_i^n| \Big\}.$$
Usually the numerical convergence is rather good and the relative order of S finally goes to 10^{-13} or so in the case of double precision computation. The obtained profile is used as the initial data $\{U_i^0\}_i$ for the test of instability.

We choose $i_{\min} = 0, i_{\max} = 1000, i_s = 100$. The choice $i_{\min} = 0, i_{\max} = 2000, i_s = 200$ is also tested. Both gives essentially the same profile.

4.3.2. Test of instability

Second we conduct two tests of instability using the data obtained above.

We see the linear stability of $\hat{U}^n \mapsto \hat{U}^{n+r}$ using E_n^{n+r}. But we need to extract some essential finite submatrix from E_n^{n+r} and choose the value of n. We choose i_- and i_+[5] so that
$$\begin{aligned} &|\rho_i^0 - \rho_L| < 10^{-4}|\rho_R - \rho_L|, i < i_-, \\ &|\rho_R - \rho_i^0| < 10^{-4}|\rho_R - \rho_L|, i > i_+ - r. \end{aligned} \quad (26)$$
Then we determine $\{4(i_+ - i_- - r)\} \times \{4(i_+ - i_- - r)\}$ matrix $\bar{E}_0^r$ by $\bar{E}_0^r = [\frac{\partial U_i^r}{\partial U_k^0}]_{i_-+r \le i \le i_+, i_- \le k \le i_+ - r}$, and numerically obtain the eigenvalue that has the largest absolute value.

We also conduct the usual two dimensional calculation by Godunov method. We test two kinds of computational domain and error triggering.

1. Computational domain is $1 \le i \le 10000, 1 \le j \le 2m$, m is a positive integer.[6] To control the error (see the footnote 2), the type of values $y_{j+\frac{1}{2}}$ and Δy on the computer program are to be "integer". The initial data $\{U_{i,j}^0\}$ are given by $\{U_i^0\}$ if $1 \le i \le 1000$, otherwise U_R. The boundaries at $i = 1, 10000$ are treated in the inflow and outflow manner, respectively. The boundaries at $j = 1, 2m$ are treated by the cyclic manner. We trigger the error by odd-even random error at $50 \le i \le 100$ of the relative order 10^{-10} or so.

[5] Practically, there is no difference in the final result of eigenvalue even if we replace 10^{-4} in (26) by 10^{-5}.

[6] There is no essential difference even if m is different. $m = 1$ is enough.

2. Computational domain is $1 \leq i \leq 10000, 1 \leq j \leq 2$. The initial data and boundary treatment are the same as the previous. The value Δy is determined so as to cause the round off error, for example, `0.7D-1`.

As far as we examined, there is no difference in the occurrence of instability between the two cases above.

4.4. Result of numerical experiments

We test various cases changing the condition. As far as our numerical experiment, the occurrence of carbuncle instability well coincides with the existence of $\bar{E}_0^r$'s eigenvalue with its absolute value exceeding 1.

We show a part of experiments' result. The part are done in a following manner.

1. The 3-shock with the characteristic $u + c$ is calculated. The parametrization $p_R/p_L = e^{\xi}$ determines the pressure ratio. $\xi < 0$ gives a shock wave. For the parametrization see [4] etc.

2. The velocity (in x-direction) is modified at the both sides of shock so that all the six characteristic speeds ($u \pm c, u$ of both sides) are positive and the ratio of the largest of them to the smallest is 10.

3. Then for $\xi = -1.0, -1.1, \cdots, -2.0$ we obtain profiles numerically with $s = \frac{1}{2} \cdot \frac{\Delta x}{\Delta t}$, and examined the linear system and two dimensional computation.

The result is shown in the following table.

ξ	Density Ratio	$i_+ - i_-$	Eigenvalue (absolute value maximum)	Occurence of carbuncle
-1.0	0.5037	37	0.9708	No
-1.1	0.4733	35	0.9779	No
-1.2	0.4455	34	0.9849	No
-1.3	0.4201	32	0.9917	No
-1.4	0.3969	31	0.9982	No
-1.5	0.3758	30	1.0044	Yes
-1.6	0.3566	29	1.0104	Yes
-1.7	0.3390	29	1.0162	Yes
-1.8	0.3231	28	1.0217	Yes
-1.9	0.3085	28	1.0269	Yes
-2.0	0.2953	27	1.0319	Yes

The table shows a good coincidence between the linear stability based on our linearization and the usual numerical computation for compressible Euler equations.

4.5. Remarks

Although the insist is not mathematically proved, it seems that numerical validation of our insist is possible. Therefore we may conclude that the carbuncle instability is caused by some kind of linear instability included in the scheme of numerical computation.

We mention that in the numerical computation of nonlinear problem the instability of computation does not always coincide with linear instability included in the nonlinear system. For example, also in the case of one dimensional computation of progressing shock wave it is possible to consider the linear system to see the amplification of small perturbation in discrete temporal evolution, but the original numerical computation is still stable even if the linear system is not stable. It is understood that the nonlinearity works to suppress the growth of instability.

Our computational validation implies that the instability caused by linear machinery grows without being suppressed by the nonlinearity. It supports the understanding that the carbuncle phenomenon is caused by some machinery existing only in multidimensional cases. There have been a dispute whether the carbuncle phenomenon is linear instability or nonlinear insta-

bility. It would be very difficult to give an correct answer to the dispute, but our numerical study gives some suggestion "the carbuncle phenomenon is basically linear instability but the instability of linear system (or the values of entries of matrix representing linear system that result instability) is from the strong nonlinearity that comes with the shock".

5. Numerical singularity in the formation of waves.

Another kind of inconvenience may be observed when waves are formed from a gap in the initial value. A similar behavior may be observed when a collision of discontinuities makes a gap from which multiple waves evolve.

We are concerned with the numerical computation by Godunov method for the Riemann problem of one dimensional compressible Euler equations (1) with the initial value

$$U(x,0)=U_0(x)\equiv\begin{cases}{}^t(\rho_-,\rho_-u_-,e_-), x<0,\\ {}^t(\rho_+,\rho_+u_+,e_+), x>0.\end{cases} \quad (27)$$

As an example of the numerical singularity, we observe the following numerical computation. The initial value of Riemann problem is the following.

$$\begin{aligned}&\rho_-=\rho_+=17.411708063,\\ &u_-=-4.560084435, u_+=4.560084435,\\ &p_-=p_+=54.59815003.\end{aligned} \quad (28)$$

where $p_\pm=(\gamma-1)\left(e_\pm-\frac{\rho_\pm(u_\pm)^2}{2}\right)$. Let the adiabatic constant $\gamma=1.4$. The exact solution has three constant states, which are

$$\begin{aligned}&(S_-)\ \rho=\rho_-, u=u_-, p=p_-,\\ &(S_0)\ \rho=1, u=0, p=1,\\ &(S_+)\ \rho=\rho_+, u=u_+, p=p_+.\end{aligned}$$

The neighboring states (S_-) and (S_0) are connected by the 1-rarefaction wave and (S_0) and (S_+) by the 3-rarefaction wave. Then the numerical computation is made with Godunov method. The number of finite volumes are 1200, and the CFL-number is 0.9. The picture shows the numerical solution when the number of time steps reaches 600.

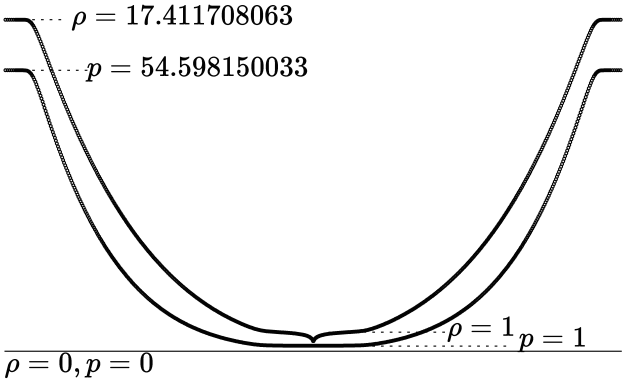

Roughly speaking the computational result has a good coincidence with the exact solution. But rather singular values are easily observed around the center. The singularity does not occur in the pressure but it clearly occurs in the density. The singularity is formed just a few steps after the start of computation. While it gets smaller until a few hundreds time steps, the singularity is completely stable at the time of picture and it never disappears nor declines.

If the convergence of scheme is discussed in the sense of L^p, the singularity does not harm with the discussion, because the nubmer of singularly valued points is uniformly finite regardless with the number of total points assumed in the discrete model. But the singularity really exists as far as we stay in the discrete model only where numerical calculation is conducted. The numerical calculation can proceed the limiting procedure only half the way but can not reach the final convergence target that is a solution of continuous model. The singular values, which are of course not physically relevant, may deteriorate the numerical result in the case of more complicated problems including reaction terms because the singular values would make the numerical estimate of reaction terms incorrect. In other words, the existence of a numerical singularity consisting of uniformly finite points could be neglected in the convergence discussion but the existence of singular value itself might do harm with the reliability of numerical computation.

Similar phenomena is observed in the case of more simple equations. We show a numerical ex-

ample for the p-system;

$$u_t + p(v)_x = 0, v_t - u_x = 0, -\infty < x < \infty, t > 0. \tag{29}$$

With $p(v) = k \cdot v^{-\gamma}$, $1 \leq \gamma \leq 3$, the p-system is a modeling of the motion of compressible gas using Lagrange coordinate. In this case, u and v mean the velocity and specific volume, respectively. Here let $k = 1, \gamma = 1.4$. We consider a Riemann problem of the following initial value.

Left state ($x < 0$): u=-3, v=1,
Right state ($x > 0$): u=3, v=1.

The following picture shows the both exact and numerical solutions of v at t=114.0958 (the number of time steps is 150). Godunov method is used to obtain the numerical solution.

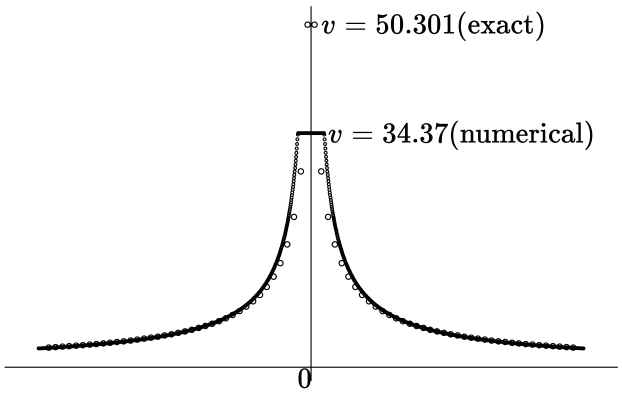

The computational region is $-40 < x < 40$, $\Delta x = 1$. The CFL-number is 0.9. In this case the analysis of discrete model is easier and it is possible to give a rough estimate of the behavior of singularity.

The both example seem alike, but there is a clear difference. This singularity disappears finally in the latter case. It seems that the main reason of this difference is that the p-system has two genuinely nonlinear characteristic fields but no linearly degenerate one. We note that three characteristic fields $u - c$, u, $u + c$ exist in the compressible Euler equations, and two $(u \pm c)$ of them are genuinely nonlinear and another (u) is linearly degenerate. On the other hand, it is easily analyzed that in the case of linear hyperbolic conservation law such a kind of singularity does not occur in the numerical calculation by Godunov method even though some smearing would be observed in a numerical result. Therefore we may conclude the following as for the numerical singularity discussed in this section.

(1) The nonlinearity of problem includes some machinery to cause numerical singularity and that it also has the machinery to erase it as the discrete temporal evolution is repeated.

(2) The coexistence of genuinely nonlinear fields and degenerated linear field in the compressible Euler equations causes some difficulty in constructing discrete models. (The nonlinearity initiates the singularity and the linearity reserves it.)

6. Conclusion

We discuss a few examples of consistency problems that lies between the continuous and discrete models. To improve the reliability of numerical simulation it is necessary to have more precise discussion on the consistency between the both models. We also need some different viewpoints of consistency other than conventional way of discussion like convergence, the order of accuracy so on.

From the viewpoint of mathematics, the coexistence of nonlinear and linear fields in the compressible Euler equations seems to give interesting problems to the numerical calculation as well as to theoretical analysis of exact solution.

References

1) H. Aiso, M. Abouziarov and T. Takahashi. Machinery of Numerical Instability in Conservative Difference Approximations for Compressible Euler Equations. . In S. Nishibata, editor, *Mathematical Analysis in Fluid and Gas Dynamics*, pages 178–191. Research Institute for Mathematical Sciences, Kyoto University, 2003.

2) J. Quirk. A contribution to the great Riemann solver debate. *International Journal*

for Numerical Methods in Fluids, 18:555–574, 1994.

3) J.-Ch. Robinet, J. Gressier, G. Casalis, and J.-M. Moschetta. Shock Wave Instability and Carbuncle Phenomenon: same intrinsic origin? . *J. Fluid Mechanics*, 417:237–263, 2000.

4) J. Smoller. *Shock waves and reaction-diffusion equations*. Springer-Verlag, NewYork, 1982.